

# Carbon–Hydrogen Bond Activation in Hydridotris(pyrazolyl)borate Complexes of Iridium

Jackson S. Wiley, Warren J. Oldham, Jr., and D. M. Heinekey\*

Department of Chemistry, University of Washington, Box 351700,  
Seattle, Washington 98195-1700

Received September 14, 1999

Methylene chloride solutions of the tris(1-pyrazolyl)borate (Tp) complexes  $\text{TpIr}(\text{PPh}_3)(\text{C}_2\text{H}_4)$  or  $\text{TpIr}(\text{C}_2\text{H}_4)_2$  react with excess  $\text{PPh}_3$  via activation of a pyrazole C–H bond to form equilibrium mixtures of  $\text{TpIr}(\text{PPh}_3)(\text{C}_2\text{H}_4)$ ,  $(N, C^5, N\text{-Tp-H})\text{Ir}(\text{PPh}_3)_2\text{H}$  (**1**), and free ethylene upon standing at room temperature. Complete conversion to **1** was accomplished by removing the displaced ethylene. The hydride complex **1** was purified by protonation at the unbound nitrogen of the pyrazole ring to afford cationic complex **2** as the  $\text{BF}_4$  salt. Deprotonation of **2** affords complex **1** in good yield and purity. The structures of **1** and **2** have been elucidated using  $^1\text{H}$  and  $^{13}\text{C}$  NMR spectroscopy. The structures of  $\text{TpIr}(\text{C}_2\text{H}_4)_2$  and complex **2** ( $\text{CH}_3\text{CN}$  solvate) been verified by X-ray crystallography. Reaction of isolated complex **1** with ethylene regenerates  $\text{TpIr}(\text{PPh}_3)(\text{C}_2\text{H}_4)$  in a reaction that is strongly inhibited by added  $\text{PPh}_3$ .

## Introduction

Rhodium and iridium complexes of hydridotris(1-pyrazolyl)borate ( $\text{TpR}^2$ ,  $\text{R} = \text{H}$  or  $\text{Me}$ )<sup>1</sup> have been studied extensively in recent years, due to their prominent role in C–H activation reactions.<sup>2–8</sup> The structure adopted by these complexes depends on the substituents on the pyrazole ring. The unsubstituted Tp ligand usually adopts a  $\kappa^3$  mode of coordination, while 3,5-dialkyl derivatives have a greater tendency to adopt the  $\kappa^2$  geometry. Within a single complex, there are several instances of observation of both structures in rapid equilibrium. An example of this situation is the recently reported study of a wide range of rhodium complexes of variously substituted Tp ligands with diene and carbonyl coligands.<sup>9</sup> It should also be pointed out that in some cases with two sterically undemanding coligands structures not apparently dictated by steric interactions are obtained. For example only  $\kappa^3\text{-Tp}^{\text{Me}_2}\text{Ir}(\text{CO})_2$  is observed for the dimethyl-substituted dicarbonyl complex, but the unsubstituted pyrazole

derivative is a roughly equimolar mixture of  $\kappa^3\text{-TpIr}(\text{CO})_2$  and  $\kappa^2\text{-TpIr}(\text{CO})_2$ .<sup>10</sup> In many cases, NMR spectroscopy does not lead to an unambiguous structural assignment of Tp complexes of the form  $\text{TpML}_2$  ( $\text{M} = \text{Rh}, \text{Ir}$ ) due to rapid dynamic process in which the three pyrazole rings are rendered equivalent on the NMR time scale. Akita and co-workers have recently demonstrated the utility of the B–H stretching vibration in the IR spectrum to distinguish between the  $\kappa^3$  and  $\kappa^2$  geometries.<sup>11</sup> In related work, Jones and co-workers have utilized  $^{11}\text{B}$  NMR spectroscopy to determine the hapticity of Tp ligands.<sup>12</sup>

The interesting reactivity in C–H activation reactions of complexes with the  $\kappa^3$  ground-state geometry has generally been attributed to the ready accessibility of a reactive  $\kappa^2$  species, although direct evidence for this is limited.<sup>13</sup> In a recent study employing very fast spectroscopy methods, Bergman and co-workers have obtained direct evidence for an “arm off” transient in photochemical alkane activation reactions of  $\text{Tp}^{\text{Me}_2}\text{Rh}(\text{CO})_2$ .<sup>8</sup>

In this work we report the observation of a novel reactivity mode of the Tp ligand which leads to formation of an iridium(III) hydride complex via activation of a C–H bond of a pyrazolyl ring. Since this reaction requires the intermediacy of a  $\kappa^2\text{-Tp}$  complex, it provides direct support for the involvement of such a species in inter- and intramolecular C–H bond activation reactions. In a preliminary account of this work,<sup>14</sup> we reported that the reaction of  $\text{TpIr}(\text{PPh}_3)(\text{C}_2\text{H}_4)$  with

(1) Substitution of the Tp ligand is represented by superscripts as suggested by Trofimenko. For example, methyl substituents in the 3,5-positions are indicated as  $\text{Tp}^{\text{Me}_2}$ . Trofimenko, S. *Chem. Rev.* **1993**, *93*, 943–980. For additional reviews of this class of complexes see: Parkin, G. *Adv. Inorg. Chem.* **1995**, *42*, 291–393. Kitajima, N.; Tolman, W. B. *Prog. Inorg. Chem.* **1995**, *43*, 418–531.

(2) Ghosh, C. K.; Graham, W. A. G. *J. Am. Chem. Soc.* **1987**, *109*, 4726–4727.

(3) Ghosh, C. K.; Rodgers, D. P. S.; Graham, W. A. G. *J. Chem. Soc., Chem. Commun.* **1988**, 1511–1512.

(4) Ghosh, C. K.; Graham, W. A. G. *J. Am. Chem. Soc.* **1989**, *111*, 375–375.

(5) Ghosh, C. K.; Hoyano, J. K.; Krentz, R.; Graham, W. A. G. *J. Am. Chem. Soc.* **1989**, *111*, 5480–5481.

(6) Jones, W. D.; Hessell, E. T. *J. Am. Chem. Soc.* **1992**, *114*, 6087–6095.

(7) Pérez, P. J.; Poveda, M. L.; Carmona, E. *Angew. Chem., Int. Ed. Engl.* **1995**, *34*, 231–233.

(8) Bromberg, S. E.; Haw, Y.; Asplund, M. C.; Lian, T.; McNamara, B. K.; Kotz, K. T.; Yeston, J. S.; Wilkens, M.; Frei, H.; Bergman, R. G.; Harris, C. B. *Science* **1997**, *278*, 260–263.

(9) Bucher, U. E.; Currao, A. Nesper, R.; Rüegger, H.; Venanzi, L. M.; Younger, E. *Inorg. Chem.* **1995**, *34*, 66–74. Bucher, U. E.; Fässler, T. F.; Hunziker, M.; Nesper, R.; Rüegger, H.; Venanzi, L. M. *Gazz. Chim. Ital.* **1995**, *125*, 181–188.

(10) Ball, R. G.; Ghosh, C. K.; Hoyano, J. K.; McMaster, A. D.; Graham, W. A. G. *J. Chem. Soc., Chem. Commun.* **1989**, 341–342.

(11) Akita, M.; Ohta, K.; Takahashi, Y.; Hikichi, S.; Moro-oka, Y. *Organometallics* **1997**, *16*, 4121–4128.

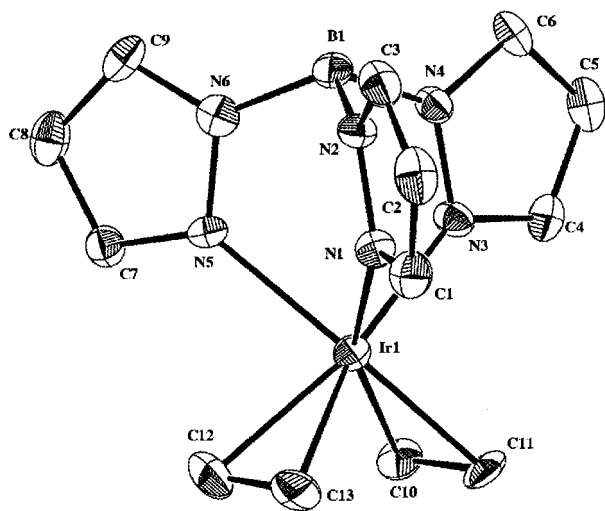
(12) Northcutt, T. O.; Lachiotte, R. J.; Jones, W. D. *Organometallics* **1998**, *17*, 5148–5152.

(13) Cf.: Gutiérrez-Puebla, E.; Monge, Á.; Nicasio, M. C.; Pérez, P. J.; Poveda, M. L.; Rey, L.; Ruiz, C.; Carmona, E. *Inorg. Chem.* **1998**, *37*, 4538–4546.

(14) Heinekey, D. M.; Oldham, W. J.; Wiley, J. S. *J. Am. Chem. Soc.* **1996**, *118*, 12842–12843.

**Table 1. Crystal Data and Structure Refinement for  $\text{TpIr}(\text{C}_2\text{H}_4)_2$  and  $2\cdot\text{CH}_3\text{CN}$** 

	$\text{TpIr}(\text{C}_2\text{H}_4)_2$	$2\cdot\text{CH}_3\text{CN}$
empirical formula	$\text{C}_{13}\text{H}_{18}\text{BIRn}_6$	$\text{C}_{47}\text{H}_{44}\text{B}_2\text{F}_4\text{IrN}_7\text{P}_2$
formula weight	461.34	1058.65
temperature, K	161(2)	161(2)
$\lambda$ , Å	0.7107	0.7107
cryst syst	monoclinic	triclinic
space group	$P2_1/n$	$P\bar{1}$
$a$ , Å	9.1637(2)	10.7907(1)
$b$ , Å	14.2015(3)	14.9708(2)
$c$ , Å	11.6283(1)	16.2606(2)
$\alpha$ , deg	90	86.2246(6)
$\beta$ , deg	104.764(1)	77.5581(8)
$\gamma$ , deg	90	85.0293(8)
volume, Å <sup>3</sup>	1463.32(5)	2403.64(5)
$Z$	4	2
$d_{\text{calc}}$ , g cm <sup>-3</sup>	2.094	1.461
no. of reflns used for indexing	536	896
abs coeff, mm <sup>-1</sup>	9.126	2.899
$F(000)$	880	1055
cryst description/color	prism/colorless	prism/colorless
cryst size	$0.27 \times 0.16 \times 0.13$ mm	$0.20 \times 0.19 \times 0.09$ mm
$2\theta$ range for data collection, deg	2.71–28.69	2.09–30.53
index ranges	$-11 \leq h \leq 12$ , $-17 \leq k \leq 17$ , $-14 \leq l \leq 14$	$-12 \leq h \leq 14$ , $-20 \leq k \leq 18$ , $-23 \leq l \leq 22$
no. of reflns collected/unique	59101/3416 [ $R(\text{int}) = 0.030$ ]	60615/13728 [ $R(\text{int}) = 0.0411$ ]
completeness to $2\theta = 28.69^\circ$	86.9%	93.3%
abs corr	SCALEPACK	face indexed
max. and min. transmission	not available	0.8052 and 0.6489
refinement method	full-matrix least-squares on $F^2$	full-matrix least-squares on $F^2$
no. of data/restraints/params	3416/0/190	13728/0/572
goodness-of-fit on $F^2$	1.072	1.064
final $R$ indices [ $I > 4\sigma(I)$ ]	$R = 0.0424$ , $R_w = 0.1102$	$R = 0.0405$ , $R_w = 0.1419$
largest diff peak and hole, e Å <sup>-3</sup>	1.625 and $-3.106$	3.508 and $-2.387$

**Figure 1.** ORTEP representation of  $\text{TpIr}(\text{C}_2\text{H}_4)_2$ . Thermal ellipsoids are shown at 50% probability. Hydrogen atoms have been omitted for clarity.

excess  $\text{PPh}_3$  affords an Ir(III) hydride complex, formulated as  $(N, C^5, N\text{-Tp-H})\text{Ir}(\text{PPh}_3)_2\text{H}$  (**1**). Complete characterization of this complex was hindered by the unavoidable presence of  $\text{PPh}_3$ , which is not readily separable from complex **1**. We now report that **1** can be protonated at the uncomplexed pyrazole nitrogen to yield a cationic complex which is readily purified and structurally characterized. Subsequent deprotonation affords pure samples of complex **1**, which has allowed for full characterization and an investigation of the mechanism of this novel C–H bond activation reaction.

## Results

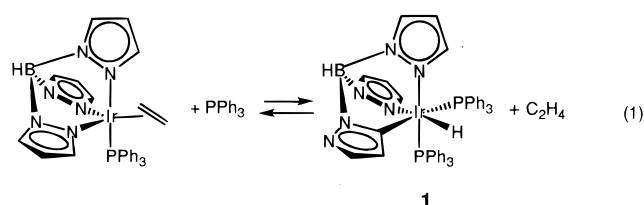
**Structure of Iridium(I) Tp Complexes.** The starting material for our synthetic work is  $\text{TpIr}(\text{C}_2\text{H}_4)_2$ . To clarify the structure of this key starting material, we

**Table 2. Selected Bond Lengths and Angles for  $\text{TpIr}(\text{C}_2\text{H}_4)_2$** 

Bond Distances (Å)			
Ir–N1	2.202(4)	Ir–C11	2.078(5)
Ir–N3	2.096(4)	Ir–C12	2.146(7)
Ir–N5	2.191(5)	Ir–C10	2.072(5)
Ir–C13	2.135(5)	C10–C11	1.445(8)
C12–C13	1.390(10)		
Bond Angles (deg)			
N3–Ir–N5	83.01(18)	N3–Ir–N1	82.83(19)
N5–Ir–N1	84.15(17)	N3–Ir–C10	88.3(2)
N1–Ir–C11	118.0(2)	N5–Ir–C10	115.3(2)
N1–Ir–C13	85.0(2)		

have examined the structure by X-ray diffraction. Crystals suitable for this purpose were grown from a saturated toluene solution. Data collection is summarized in Table 1. An ORTEP diagram and key structural features are given in Figure 1 and Table 2, respectively. Details of the structure solution and refinement are included in the Experimental Section. The Tp ligand is coordinated in a  $\kappa^3$  fashion.

**Reactions with  $\text{PPh}_3$ .** Reaction of excess  $\text{PPh}_3$  with  $\text{TpIr}(\text{C}_2\text{H}_4)_2$  or  $\text{TpIr}(\text{PPh}_3)(\text{C}_2\text{H}_4)$  in methylene chloride solution affords equilibrium mixtures of  $\text{TpIr}(\text{PPh}_3)(\text{C}_2\text{H}_4)$ ,<sup>15</sup> the hydride complex  $(N, C^5, N\text{-Tp-H})\text{Ir}(\text{PPh}_3)_2\text{H}$  (**1**), and free ethylene upon standing for 20 h (eq 1). No intermediates were detected.



(15) Oldham, W. J.; Heinekey, D. M. *Organometallics* **1997**, *16*, 467–474.

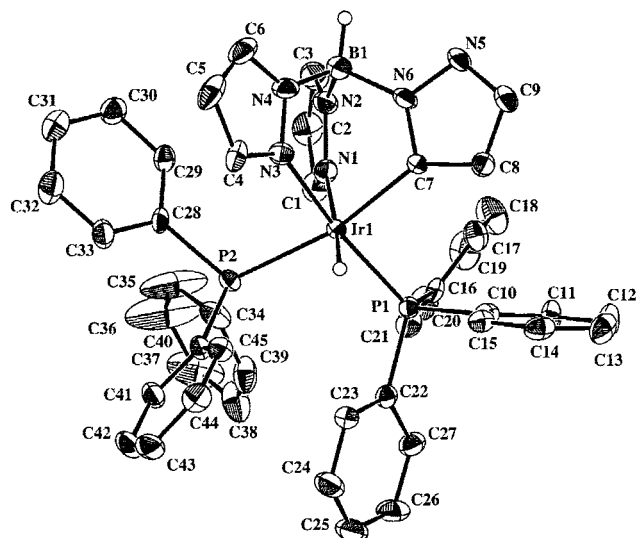
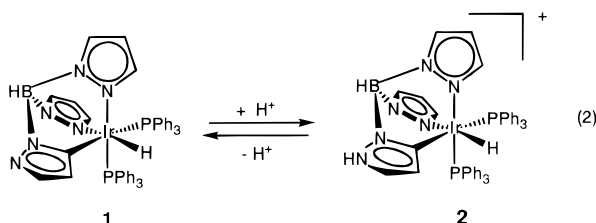


**Figure 2.** ORTEP representation of the cation of complex **2**. Thermal ellipsoids are shown at 50% probability. Hydrogen atoms have been omitted for clarity.

Complete conversion to complex **1** was achieved by reaction with a 10-fold excess of phosphine combined with periodic purging of the reaction mixture with argon, which serves to remove the byproduct ethylene. Under these conditions, complex **1** was obtained in a state of reasonable purity, but contamination with  $\text{PPh}_3$  hindered complete characterization. Purification was accomplished by protonation ( $\text{HBF}_4 \cdot \text{Et}_2\text{O}$ ), which occurs at the free nitrogen atom of the activated ring to afford the cationic complex **2** (eq 2).



Deprotonation of **2** is readily achieved by reaction with aqueous sodium hydroxide in methylene chloride to afford samples of **1** in a state of high purity. Complex **1** was characterized by  $^{31}\text{P}$ ,  $^1\text{H}$ , and  $^{13}\text{C}$  NMR spectroscopy as well as infrared spectroscopy.

For complex **2**, similar spectroscopic data were obtained, consistent with the formulation shown above. The structure of **2** was confirmed by X-ray crystallography (see below).

**Solid-State Structure of Complex 2.** Colorless crystals of  $2 \cdot \text{CH}_3\text{CN}$  suitable for X-ray diffraction were grown by slow diffusion of diethyl ether into a concentrated acetonitrile solution. Complex **2** is air stable in this form. An ORTEP diagram of the iridium cation and key structural features are given in Figure 2 and Table 3, respectively. Details of the structure solution and refinement are included in the Experimental Section.

**Phosphine Exchange Reactions.** Complex  $1\text{-}d_{30}$  shows exchange with free nondeuterated triphenyl phosphine ( $t_{1/2} = 48$  h; phosphine concentration ca. 0.01 M), while complex **2** shows no exchange. Monitoring the reaction of complex **1** in  $\text{CD}_2\text{Cl}_2$  with  $\text{PPh}_3\text{-}d_{15}$  by  $^{31}\text{P}\{^1\text{H}\}$  NMR spectroscopy shows that the initial set of

**Table 3.** Selected Bond Lengths and Angles for  $2 \cdot \text{CH}_3\text{CN}$

Bond Distances (Å)			
Ir–N1	2.190(4)	Ir–P1	2.2874(11)
Ir–N3	2.108(4)	Ir–P2	2.3971(11)
Ir–C7	2.098(4)	Ir–H	1.52(7)
Bond Angles (deg)			
C7–Ir–N1	85.95(16)	N3–Ir–P1	169.95(11)
C7–Ir–N3	82.57(16)	N3–Ir–P2	86.24(11)
N1–Ir–N3	88.89(15)	C7–Ir–H	97(3)
P1–Ir–P2	101.16(4)	N1–Ir–H	177(3)
C7–Ir–P1	90.56(12)	N3–Ir–H	90(3)
C7–Ir–P2	167.76(12)	P1–Ir–H	84(3)
N1–Ir–P1	97.96(11)	P2–Ir–H	88(3)
N1–Ir–P2	88.89(11)		

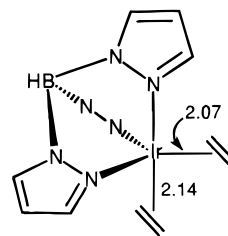
two doublet resonances at 3.80 and 1.02 ppm was augmented by a new doublet resonance at 3.32 ppm. This is consistent with exchange of only one of the two phosphine ligands. The labile phosphine ligand is the one trans to the metalated carbon (see discussion).

Dissolution of complex **1** in acetonitrile leads to a new complex and displacement of  $\text{PPh}_3$ . Spectroscopic data is consistent with the replacement of the phosphine trans to the metalated carbon with acetonitrile (see Discussion). The rate of replacement of phosphine in complex **1** with acetonitrile is similar to the rate of phosphine exchange.

**Reaction of Complex 1 with Ethylene.** Complex **1** reacts with ethylene (1 atm, room temperature) to reform the Ir(I) complex  $\text{TpIr}(\text{C}_2\text{H}_4)_2\text{PPh}_3$ . This reaction proceeds to completion in 72 h. When the reaction was carried out in the presence of 10 equiv of  $\text{PPh}_3$ , the reaction was only 20% complete after 3 days. In the presence of 20 equiv of  $\text{PPh}_3$ , the reaction was only 5% complete after 3 days.

## Discussion

**Structure of  $\text{TpIr}(\text{C}_2\text{H}_4)_2$ .** The solid-state structure of  $\text{TpIr}(\text{C}_2\text{H}_4)_2$  is very similar to that of  $\text{TpIr}(\text{COD})$ ,<sup>16</sup> with N–Ir–N angles in the Tp ligand between  $81^\circ$  and  $84^\circ$ . The Ir–C bond distances in the axial ethylene ligand (trans to a pyrazole nitrogen) are longer (by ca. 0.1 Å) than those to the equatorial ethylene (see below).



The bond distances of 2.072(5) and 2.078(5) Å between Ir and the ethylene carbons in the equatorial position should be compared with the similar distances of 2.06(2) and 2.10(2) Å recently reported by Carmona and co-workers in the related complex  $\text{Tp}^{\text{Me}_2}\text{Ir}(\text{PMe}_2\text{-Ph})(\text{C}_2\text{H}_4)$ .<sup>13</sup> Our structure of  $\text{TpIr}(\text{C}_2\text{H}_4)_2$  also resembles closely the previously reported results for  $\text{Tp}^{\text{Me}_2}\text{Ir}(\text{C}_2\text{H}_4)_2$ .<sup>17</sup>

(16) Albinati, A.; Bovens, M.; Rüegger, H.; Venanzi, L. M. *Inorg. Chem.* **1997**, *36*, 5991–5999.

(17) Alvarado, Y.; Boutry, O.; Gutiérrez, E.; Monge, Á.; Nicasio, M. C.; Poveda, M. L.; Pérez, P. J.; Ruiz, C.; Bianchini, C.; Carmona, E. *Chem. Eur. J.* **1997**, *3*, 860–873.



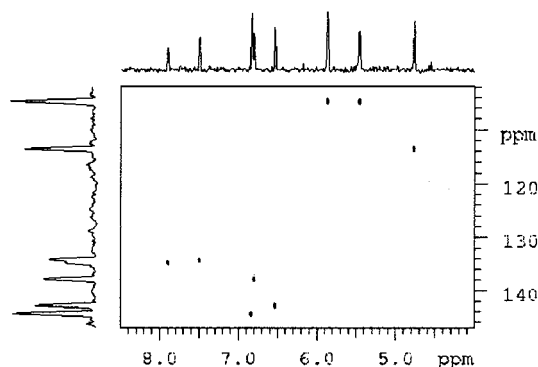


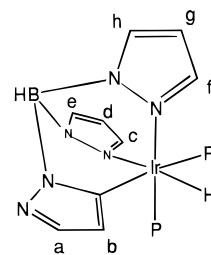
**Figure 3.** HMQC spectrum of complex **1-d<sub>30</sub>**. Atom labels are defined in the text.

The question of solution-state structure of complexes of this type has been addressed by Akita and co-workers, who find that the B–H stretch in the infrared spectrum is diagnostic of  $\kappa^2$  versus  $\kappa^3$  coordination of the Tp ligand.<sup>11</sup> In the case of  $\text{TpIr}(\text{C}_2\text{H}_2)_2$ , only a single B–H stretch at  $2478\text{ cm}^{-1}$  (chloroform solution) has been observed,<sup>18</sup> which is consistent with retention of the  $\kappa^3$  structure in solution, in line with previous suggestions by Carmona and co-workers.<sup>17</sup> Thus  $\text{Tp}^{\text{Me}_2}\text{Ir}(\text{C}_2\text{H}_4)_2$  and  $\text{TpIr}(\text{C}_2\text{H}_4)_2$  adopt the  $\kappa^3$  mode of coordination both in the solid state and in solution. In contrast, the dicarbonyl complexes reported by Graham and co-workers give both  $\kappa^2$  and  $\kappa^3$  structures with the unsubstituted pyrazole ligand, but methyl substitution favors the  $\kappa^3$  structure.<sup>10</sup>

**Synthesis and Characterization of (*N,C<sup>5</sup>,N-p-H*)- $\text{HIr}(\text{PPh}_3)_2$  (**1**).** Complex **1** can be formed in good yield from  $\text{TpIr}(\text{C}_2\text{H}_4)_2$  or  $\text{TpIrPPh}_3(\text{C}_2\text{H}_4)$  by reaction with excess  $\text{PPh}_3$ . In the  $^1\text{H}$  NMR spectrum of **1**, a hydride resonance at  $-18.95\text{ ppm}$  is observed which exhibits coupling to two  $^{31}\text{P}$  nuclei ( $J_{\text{HP}} = 12\text{ Hz}, 20\text{ Hz}$ ). When the reaction was carried out with  $\text{PPh}_3\text{-}d_{15}$ , the same hydride resonance was observed in the  $^1\text{H}$  NMR spectrum of **1-d<sub>30</sub>**. Consistent with the presence of two different phosphine ligands, the  $^{31}\text{P}$  NMR spectrum shows two resonances at  $3.80$  and  $1.02\text{ ppm}$ , with coupling  $J_{\text{PP}} = 10\text{ Hz}$ .

Since vinyl C–H activation is well preceded in Tp complexes of iridium,<sup>17</sup> the possibility that the hydride ligand results from activation of the bound ethylene must be considered. This hypothesis is ruled out by the absence of vinylic resonances in the  $^1\text{H}$  NMR spectrum.

Convincing evidence for activation of a pyrazole C–H bond is provided by the observation of eight different resonances of equal intensity for the pyrazole ring protons in the  $^1\text{H}$  NMR spectrum of **1-d<sub>30</sub>**. The assignments of the proton resonances shown below were determined by examination of proton–proton couplings and by a series of NOE experiments. For example, irradiation of the hydride signal produced a decreased intensity for two signals assigned as  $\text{H}_b$  and  $\text{H}_f$ . These assignments were verified by a 2D COSY experiment. To identify the  $^{13}\text{C}$  chemical shifts, a 2D HMQC (heteronuclear multiple quantum coherence) experiment was performed (Figure 3). This allowed for assignment of all pyrazole carbons except for the metalated Ir bound carbon atom.



An HMBC (heteronuclear multiple bond correlation) experiment was carried out in order to locate the resonance due to the metalated carbon by observing all the carbon resonances coupled to protons by more than one bond. Long-range coupling was observed primarily to the Ir–H resonance, which showed an intense cross-peak to a doublet of doublets at  $132\text{ ppm}$ . This was confirmed with more distant couplings to  $\text{H}_a$  and  $\text{H}_b$ . A high S/N  $^{13}\text{C}$  spectrum confirmed the presence of a doublet of doublets at  $132\text{ ppm}$ , which is difficult to observe under normal conditions due to the coupling to two phosphorus nuclei and lack of an attached hydrogen. The resonance due to the metalated carbon is found near other pyrazole ring signals, suggesting that coordination of carbon to iridium rather than hydrogen has surprisingly little effect on the  $^{13}\text{C}$  chemical shift. The two distinct couplings ( $12$  and  $98\text{ Hz}$ ) of the metalated carbon to  $^{31}\text{P}$  are only consistent with a structure having one phosphine ligand trans to this carbon and one cis. The larger coupling is attributed to the trans phosphine.

Repeating the above experiments with samples prepared from protio triphenyl phosphine allowed assignment of the phenyl ring carbon and proton signals. Two distinct phenyl ring environments were detected, and these were assigned as Ph and Ph' (see Experimental Section).

**Synthesis and Characterization of [(*N,C<sup>5</sup>,N-Tp*)- $\text{HIr}(\text{PPh}_3)_2$ ] $\text{BF}_4$  (**2**).** Protonation of complex **1** occurs at the nitrogen atom of the metalated pyrazole ring to afford cationic complex **2**, which is readily separable by recrystallization from the excess of  $\text{PPh}_3$  present in samples of **1** prepared as above. Diagnostic of protonation at nitrogen is the slightly broadened resonance in the  $^1\text{H}$  NMR spectrum at  $12.1\text{ ppm}$ . Other  $^1\text{H}$  and  $^{13}\text{C}$  resonances are similar to those observed for complex **1**. A similar set of NOE and 2D NMR experiments confirmed the proton and carbon resonance assignments.

The protonation/deprotonation reaction that interconverts complexes **1** and **2** is rapid on the NMR time scale. The  $^1\text{H}$  NMR spectrum of an equimolar mixture of **1** and **2** in  $\text{CD}_2\text{Cl}_2$  or  $\text{CD}_3\text{CN}$  gives a very broad N–H proton resonance and exhibits a single set of hydride and pyrazole resonances, which are at frequencies intermediate between the values observed for **1** and **2**. Similar observations were made in the  $^{31}\text{P}$  NMR spectrum of the mixture. These spectra are independent of temperature down to  $230\text{ K}$ . These observations are consistent with rapid intermolecular proton exchange between **1** and **2**.

Deprotonation of complex **2** with excess aqueous sodium hydroxide in methylene chloride solution affords samples of **1** in a state of high purity.

**Solid-State Structure of  $2\cdot\text{CH}_3\text{CN}$ .** An ORTEP drawing of the iridium cation and key bond lengths and angles are given in Figure 2 and Table 2, respectively.

(18) Tanke, R. S.; Crabtree, R. H. *Inorg. Chem.* **1989**, *28*, 3444–3447.

The structure of the cation is approximately octahedral, with the ligand-to-ligand angles all between 80° and 100°. The iridium hydride was located and refined with an Ir–H distance of 1.52 Å. This is somewhat shorter than the expected distance of 1.6–1.7 Å and likely reflects the commonly observed underestimation of M–H distances in X-ray diffraction experiments. The two Ir–N bond distances are 2.11 and 2.19 Å, with the longer one being trans to the hydride. The metalated carbon Ir–C bond distance is 2.10 Å, not significantly different from the shorter of the two N–Ir bond distances. The two Ir–P distances are significantly different (2.29 and 2.40 Å), with the longer one trans to carbon, consistent with the structural assignment presented here. One of the triphenylphosphine rings suffers from some disorder; however this does not greatly impact the refinement of the structure, as the final *R* value is 4%. An alternative structural model that places the metalated ring trans to the hydride affords a slightly higher *R* of 4.2%. The NMR data discussed above for **1** and **2** explicitly support formulation of the complex with the hydride cis to the carbon, in that the metalated carbon atom was shown to be cis to one phosphine and trans to the other phosphine ligand. This requires that the Ir bound carbon be cis to the hydride ligand.

**Reactivity of Complexes 1 and 2.** While complex **2** is indefinitely stable in solution at room temperature, complex **1** undergoes decomposition in methylene chloride solution ( $t_{1/2}$  ca. 48 h) to afford a mixture of several products. The major product exhibits a hydride resonance at –18.7 ppm in the  $^1\text{H}$  NMR spectrum which exhibits coupling to three phosphine ligands. This signal is very similar to the hydride resonances reported by Bennett and Milner<sup>19</sup> for the orthometalated species derived from  $\text{IrCl}(\text{PPh}_3)_3$ . This hydride resonance was not observed in the decomposition of samples of **1-*d*<sub>30</sub>**, which confirms that this hydride arises from orthometallation of a phosphine ligand.

In contrast to the multiple products observed in methylene chloride solution, dissolution of **1** in acetonitrile initially affords a single product. NMR spectra of this complex are consistent with the presence of a hydride and a single  $\text{PPh}_3$  ligand. The low symmetry of the pyrazole resonances indicates retention of the metalated pyrazole ring. In the HMBC spectrum, a cross-peak to the Ir–H resonance was observed as a doublet at 121.8 ppm with  $J_{\text{CP}} = 12$  Hz. Thus the remaining  $\text{PPh}_3$  ligand is cis to the Ir–C and the acetonitrile is trans to the Ir–C. This conclusion is based on the attribution of the smaller of the two couplings observed in **1** and **2** between the metalated carbon and the  $^{31}\text{P}$  nuclei of the phosphine ligands to the cis phosphine. The structure of this product is assigned as the acetonitrile complex (*N,C<sup>5</sup>,N*-Tp-H) $\text{IrH}(\text{PPh}_3)(\text{NCCH}_3)$ , with the acetonitrile trans to the metalated carbon. The formation of this acetonitrile adduct from **1** indicates lability of only the phosphine ligand trans to the C-bound pyrazole ring. Prolonged reaction with acetonitrile leads to a complex mixture of products. In contrast, the cationic complex **2** is indefinitely stable in acetonitrile.

**Phosphine Exchange Reactions.** Complex **1-*d*<sub>30</sub>** shows exchange with free nondeuterated triphenyl

phosphine ( $t_{1/2} = 48$  h), while complex **2** shows no exchange. The rate of replacement of phosphine in complex **1** with acetonitrile is similar to the rate of phosphine exchange. The lack of phosphine ligand exchange in complex **2** is consistent with the lack of reaction of this complex with acetonitrile. The reaction of complex **1** with  $\text{PPh}_3\text{-}d_{15}$  leads to exchange of only one phosphine, as indicated by the appearance of one new doublet signal in the  $^{31}\text{P}\{^1\text{H}\}$  NMR spectrum. This arises from the small isotope effect on the  $^{31}\text{P}$  chemical shifts caused by deuteration of the aryl rings. Thus complex **1** exhibits an AB pattern in the  $^{31}\text{P}\{^1\text{H}\}$  NMR spectrum with chemical shifts of 3.80 and 1.02 ppm and  $J = 10$  Hz. When one  $\text{PPh}_3\text{-}d_{15}$  is incorporated, signals at 3.32 and 1.02 ppm are observed, with the same coupling. Based on the acetonitrile reaction described above, the labile phosphine is trans to the Ir–C bond of the metalated pyrazole ring.

**Mechanism of Formation of 1.** The reaction depicted in eq 1 is readily reversible, indicating that the six-coordinate Ir(III) hydride and the five-coordinate Ir(I) olefin phosphine complex are quite similar in overall stability. In the absence of excess phosphine,  $\text{TpIrPPh}_3\text{-(C}_2\text{H}_4\text{)}$  does not undergo pyrazole ring activation. Carmona and co-workers have noted that the closely related complexes  $\text{Tp}^{\text{Me}_2}\text{Ir}(\text{PR}_3)(\text{C}_2\text{H}_4)$  will give Ir(III) vinyl hydride species upon mild heating. The driving force for reactions of this type is provided by the formation of strong Ir–H and Ir–C bonds, as noted for the many reported examples of intermolecular alkane activation by Ir(I) complexes. It is instructive to consider the requirements for these alkane activation reactions and to examine some cases where thermal alkane activation does not occur. For example,  $\text{TpIr}(\text{CO})_2$  exhibits both the  $\kappa^2$  and  $\kappa^3$  structures in solution, but requires photoextrusion of a CO ligand in order to activate alkanes.<sup>20</sup> Consistent with these observations, the work of Goldberg and Wick<sup>21</sup> on Pt(II) complexes clearly demonstrates that a three-coordinate intermediate  $\kappa^2\text{-Tp}^{\text{Me}_2}\text{PtMe}$  is the immediate precursor to alkane activation. If the same mechanism operates in our iridium complexes, dechelation of a pyrazole ring and loss of a phosphine ligand may be required for activation of the C–H bond of the pyrazole ring.

We had previously suggested the intermediacy of  $\kappa^3\text{-TpIr}(\text{PPh}_3)_2$  in the formation of complex **1**. This proposal is based on the observation that Tp complexes of Ir(III) with olefin ligands are inert to displacement of the olefin under thermal conditions. In a previous study of the reaction of  $\kappa^3\text{-TpIr}(\text{PPh}_3)(\text{C}_2\text{H}_4)$  with hydrogen, kinetic evidence showed that addition of excess ethylene did not slow the reaction to form  $\kappa^3\text{-TpIr}(\text{PPh}_3)\text{H}_2$ . Thus the Ir(III) complex (*N,C<sup>5</sup>,N*-Tp) $\text{Ir}(\text{PPh}_3)(\text{C}_2\text{H}_4)\text{H}$  is ruled out as an intermediate in the formation of **1**.

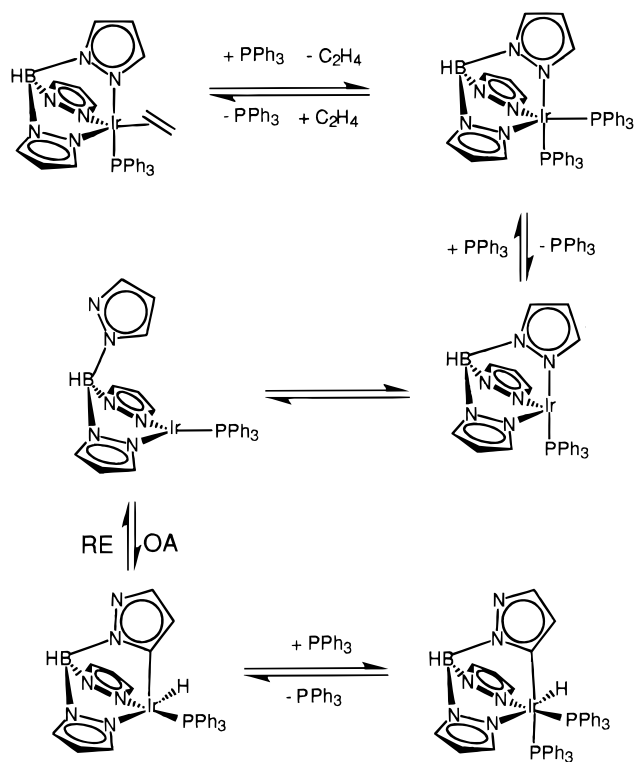
The formation of complex **1** from  $\text{TpIr}(\text{PPh}_3)(\text{C}_2\text{H}_4)$  occurs upon addition of  $\text{PPh}_3$ . Incorporation of the second  $\text{PPh}_3$  ligand leads to extrusion of ethylene and the presumed formation of an intermediate with a greater tendency to oxidatively add a C–H bond. Based

(20) Hoyano, J. K.; Graham, W. A. G. *Abstracts of Papers Part I*. Third Chemical Congress of North America, Toronto, Canada; American Chemical Society: Washington, DC, 1988; INOR 216.

(21) Wick, D. D.; Goldberg, K. I. *J. Am. Chem. Soc.* **1997**, *119*, 10235–10236.

(19) Bennett, M. A.; Milner, D. L. *J. Am. Chem. Soc.* **1969**, *91*, 6983–6994.

Scheme 1



on the observations of Goldberg and Wick,<sup>21</sup> we suggest that the immediate precursor to metalated complex **1** is  $\kappa^2$ -TpIr(PPh<sub>3</sub>), which oxidatively adds a pyrazole C–H bond to give  $(N,C^5,N\text{-Tp})\text{HIr}(\text{PPh}_3)$  and then incorporates a second phosphine ligand to afford **1**. This postulated mechanism is consistent with our observation that complex **1** readily incorporates deuterated phosphine. Important evidence for this mechanism is the observation that the reaction of **1** with ethylene is strongly inhibited by the presence of PPh<sub>3</sub>. A summary of the proposed mechanism for the C–H activation reaction is given in Scheme 1.

In contrast to the apparent instability of TpIr(PPh<sub>3</sub>)<sub>2</sub>, Hill and co-workers have reported that TpRh(PPh<sub>3</sub>)<sub>2</sub> can be prepared from the reaction of ClRh(PPh<sub>3</sub>)<sub>3</sub> with KTp.<sup>22</sup> Seeking direct evidence for the postulated TpIr(PPh<sub>3</sub>)<sub>2</sub>, we attempted the reaction of ClIr(PPh<sub>3</sub>)<sub>3</sub> with KTp. A plethora of products was obtained, including species with hydride resonances consistent with orthometalation of PPh<sub>3</sub> ligands.<sup>19</sup>

We had previously reported that the Ir(III) dihydrogen hydride complex [TpIrH(H<sub>2</sub>)PPh<sub>3</sub>]<sup>+</sup> exchanges hydrogen with deuterium gas.<sup>23</sup> A plausible alternative route to complex **2** was envisaged via displacement of hydrogen from [TpIrH(H<sub>2</sub>)PPh<sub>3</sub>]<sup>+</sup> with PPh<sub>3</sub>. When this reaction was carried out with a range of PPh<sub>3</sub> concentrations, the main product of the reaction was TpIrH<sub>2</sub>-PPh<sub>3</sub>, arising from proton transfer to PPh<sub>3</sub>. Moderate amounts of other hydride products were detected by <sup>1</sup>H NMR. Approximately 5% of the product could be attributed to complex **2**, providing evidence for an alternative pathway to metalated products.

## Conclusion

Activation of unreactive C–H bonds of a pyrazole ring in Ir complexes under mild conditions has been observed. A stable Ir(III) hydride complex resulting from pyrazole C–H bond activation has been isolated, and the crystal structure of a protonated derivative has been determined. The Ir(I) complex TpIr(PPh<sub>3</sub>)<sub>2</sub> is believed to be an intermediate in the C–H bond activation chemistry, but cannot be prepared by methods that succeed for the rhodium analogue. Phosphine inhibition experiments suggest that the immediate precursor to the C–H bond activated product is a three-coordinate monophosphine complex with a  $\kappa^2$ -Tp ligand. This work suggests that the key requirement for thermal C–H bond activation reactions in TpIr(I) complexes is the accessibility of a three-coordinate species with a  $\kappa^2$ -Tp ligand. Such three-coordinate species are not thermally accessible in the case of dicarbonyl complexes of Ir.

## Experimental Section

**General Procedures.** Unless stated otherwise, all preparations and manipulations were carried out under argon following conventional Schlenk techniques. Solvents were dried and degassed before use. TpIr(C<sub>2</sub>H<sub>4</sub>)<sub>2</sub> was prepared by the procedure of Crabtree and Tanke.<sup>18</sup> PPh<sub>3</sub>-d<sub>15</sub> was prepared by the reaction of C<sub>6</sub>D<sub>5</sub>MgBr with PCl<sub>3</sub>. Microanalyses were by Canadian Microanalytical. Infrared spectra were recorded on a Perkin-Elmer model 1600 spectrometer. NMR spectra were recorded on Bruker AC-200, DPX-200, AF-300, DRX-499, and AM-500 spectrometers. The <sup>1</sup>H and <sup>13</sup>C spectra were referenced to the solvent resonance; chemical shifts are reported relative to TMS. <sup>31</sup>P chemical shifts were referenced to external 85% H<sub>3</sub>PO<sub>4</sub>.

**Solid-State Structure of TpIr(C<sub>2</sub>H<sub>4</sub>)<sub>2</sub>.** Crystals were grown from concentrated toluene solution and mounted on glass capillaries in oil. Diffraction measurements were made on a colorless prismatic crystal of dimensions 0.27 × 0.16 × 0.13 mm in a nitrogen stream at 161 K on a Nonius KappaCCD diffractometer using graphite-monochromated radiation ( $\lambda$  = 0.71070 Å). Crystal-to-detector distance was 27 mm, and exposure time was 15 s for all sets. The scan width was 1°. Data collection was 86.9% complete to 28.69° in 2 $\theta$ . A total of 59 101 partial and complete reflections were collected covering the indices  $h$  = –11 to 12,  $k$  = –17 to 17,  $l$  = –14 to 14. A total of 3416 reflections were symmetry independent, and the  $R_{\text{int}}$  = 0.030 indicated good data quality. Indexing and unit cell refinement, based on 536 reflections, indicated a monoclinic P lattice. The space group was  $P2_1/n$  with cell parameters  $a$  = 9.1637(2) Å,  $b$  = 14.2015(3) Å,  $c$  = 11.6283(1) Å;  $\alpha$  =  $\gamma$  = 90°,  $\beta$  = 104.764°. The cell volume was 1463.32(5) Å<sup>3</sup>, and the calculated density was 2.094 g/cm<sup>3</sup>, with  $Z$  = 4. Solution by direct methods produced a complete heavy atom phasing model consistent with the proposed structure. All hydrogen atoms were placed with idealized geometry except for H1B (boron hydrogen), which was located by difference Fourier synthesis. Hydrogen atoms were refined with a riding model with  $U_{\text{iso}}$  values fixed at 1.1  $U_{\text{eq}}$  of their parent atom.

**[(N,C<sup>5</sup>,N-Tp)HIr(PPh<sub>3</sub>)<sub>2</sub>]BF<sub>4</sub> (**2**).** TpIr(C<sub>2</sub>H<sub>4</sub>)<sub>2</sub> (200 mg, 0.44 mmol) and PPh<sub>3</sub> (1.14 g, 4.4 mmol) were combined in a glass reactor equipped with a Kontes vacuum valve. Dichloromethane (2 mL) was added by vacuum transfer. Upon thawing, all solids dissolved and the rapid evolution of ethylene was observed. After purging with argon, the reaction mixture was allowed to stand for 20 h. HBF<sub>4</sub> (54% in Et<sub>2</sub>O; 79  $\mu$ L, 1 equiv) was added and the solution was mixed. A white powder precipitated upon addition of diethyl ether and was filtered in air on a Buchner funnel. Yield: 293 mg, 76%. Anal. Calcd for C<sub>45</sub>H<sub>41</sub>B<sub>2</sub>F<sub>4</sub>N<sub>6</sub>P<sub>2</sub>: C, 53.12; H, 4.06; N, 8.26. Found: C,

(22) Hill, A. F.; White, A. J. P.; Williams, D. J.; Wilton-Ely, J. D. E. *T. Organometallics* **1998**, *17*, 3152–3154.

(23) Oldham, W. J.; Hinkle, A. S.; Heinekey, D. M. *J. Am. Chem. Soc.* **1997**, *119*, 11028–11036.



52.99; H, 4.20; N, 8.12.  $^1\text{H}$  NMR (500 MHz,  $\text{CD}_2\text{Cl}_2$ ): 12.1 (br, 1H, N–H<sup>+</sup>); 7.90 (d, 1H, H<sub>e</sub>); 7.53 (m, 1H, H<sub>h</sub>); 7.34 (m, 2H, Ph<sub>para</sub>); 7.28 (m, 2H, Ph<sub>para</sub>); 7.27 (m, 4H, Ph<sub>meta</sub>); 7.15 (dt, 4H,  $J = 2.4$  Hz, 8 Hz, Ph<sub>meta</sub>); 7.11 (br, 1H, H<sub>a</sub>); 7.10 (dt, 4H,  $J = 3$  Hz, 8 Hz, Ph<sub>ortho</sub>); 6.87 (m, 4H, Ph<sub>ortho</sub>); 6.84 (m, 1H, H<sub>i</sub>); 6.25 (d, 1H, H<sub>c</sub>); 5.88 (t, 1H, H<sub>d</sub>); 5.52 (t, 1H, H<sub>g</sub>); 5.15 (m, 1H, H<sub>b</sub>); –18.91 (dd,  $J_{\text{HP}} = 12$  Hz, 20 Hz, H–Ir).  $^{31}\text{P}\{\text{sel } ^1\text{H}\}$ : 2.92 (dd,  $J_{\text{PP}} = 14$  Hz,  $J_{\text{PH}} = 12$  Hz); –1.33 (dd,  $J_{\text{PP}} = 14$  Hz,  $J_{\text{PH}} = 20$  Hz).  $^{13}\text{C}\{^1\text{H}\}$ : 146.1 (s, C<sub>f</sub>); 145.1 (dd,  $J_{\text{CP}}(\text{cis}) = 11$  Hz,  $J_{\text{CP}}(\text{trans}) = 103$  Hz, C–Ir); 144.0 (s, C<sub>e</sub>); 136.4 (s, C<sub>e</sub>); 136.0 (s, C<sub>h</sub>); 133.9 (d,  $J_{\text{CP}} = 11$  Hz, Ph<sub>ortho</sub>); 133.7 (d,  $J_{\text{CP}} = 9$  Hz, Ph<sub>meta</sub>); 132.7 (d,  $J_{\text{CP}} = 57$  Hz, Ph<sub>ipso</sub>); 131.5 (d,  $J_{\text{CP}} = 44$  Hz, Ph<sub>ipso</sub>); 130.6 (s, Ph<sub>para</sub>); 130.4 (d,  $J_{\text{CP}} = 4$  Hz, C<sub>a</sub>); 128.7 (d,  $J_{\text{CP}} = 9$  Hz, Ph<sub>meta</sub>); 128.5 (d,  $J_{\text{CP}} = 11$  Hz, Ph<sub>ortho</sub>); 117.2 (d,  $J_{\text{CP}} = 4$  Hz, C<sub>b</sub>); 106.4 (s, C<sub>g</sub>); 106.2 (s, C<sub>d</sub>). IR (Nujol,  $\text{cm}^{-1}$ ): 2478 ( $\nu_{\text{BH}}$ ), 2185 ( $\nu_{\text{IrH}}$ ).

Complex **2** was also formed in the reaction of  $\text{PPh}_3$  with  $[\text{TpIrH}(\text{H}_2)\text{PPh}_3]\text{BF}_4$ , although in very low yield. Colorless crystals of **2** suitable for X-ray diffraction were grown by slow diffusion of diethyl ether into a concentrated acetonitrile solution. Complex **2** is air stable in this form.

**(*N,C<sup>5</sup>,N-Tp-H*)Ir(PPh<sub>3</sub>)<sub>2</sub> (1).** Complex **2** (50 mg, 0.05 mmol) was dissolved in  $\text{CH}_2\text{Cl}_2$  (5 mL) and extracted 3 times with aqueous NaOH (10 mL, 1 M) and then with  $3 \times 10$  mL of deionized water. The  $\text{CH}_2\text{Cl}_2$  solution was evaporated to dryness and solid **1** isolated as a pale yellow air-stable solid (29 mg, 64%). Anal. Calcd for  $\text{C}_{45}\text{H}_{40}\text{IrN}_6\text{P}_2$ : C, 58.14; H, 4.34; N, 9.04. Found: C, 57.66; H, 4.44; N, 8.86.  $^1\text{H}$  NMR (500 MHz,  $\text{CD}_2\text{Cl}_2$ ): 7.86 (d, 1H, H<sub>e</sub>); 7.47 (m, 1H, H<sub>h</sub>); 7.28 (m, 2H, Ph<sub>para</sub>); 7.25 (m, 4H, Ph<sub>meta</sub>); 7.20 (m, 2H, Ph<sub>para</sub>); 7.10 (dt, 4H,  $J = 2$  Hz, 8 Hz, Ph<sub>ortho</sub>); 7.03 (dt, 4H,  $J = 2$  Hz, 8 Hz, Ph<sub>ortho</sub>); 6.89 (m, 4H, Ph<sub>meta</sub>); 6.78 (m, 1H, H<sub>a</sub>); 6.80 (m, 1H, H<sub>i</sub>); 6.54 (d, 1H, H<sub>e</sub>); 5.83 (t, 1H, H<sub>d</sub>); 5.43 (t, 1H, H<sub>g</sub>); 4.76 (t, 1H, H<sub>b</sub>); –18.95 (dd,  $J_{\text{HP}} = 10$  Hz, 20 Hz, 1H, H–Ir).  $^{31}\text{P}\{\text{aromatic } ^1\text{H}\}$ : 3.80 (dd,  $J_{\text{PP}} = 10$  Hz,  $J_{\text{PH}} = 10$  Hz); 1.02 (dd,  $J_{\text{PP}} = 10$  Hz,  $J_{\text{PH}} = 20$  Hz).  $^{13}\text{C}\{^1\text{H}\}$ : 144.9 (C<sub>a</sub>); 143.6 (C<sub>e</sub>); 138.6 (d,  $J_{\text{CP}} = 8.5$  Hz, C<sub>f</sub>); 135.3 (C<sub>e</sub>); 134.7 (d,  $J_{\text{CP}} = 56$  Hz, Ph<sub>ipso</sub>); 134.6 (d,  $J_{\text{CP}} = 40$  Hz, Ph<sub>ipso</sub>); 133.9 (d,  $J_{\text{CP}} = 9$  Hz, Ph<sub>meta</sub>); 133.8 (d,  $J_{\text{CP}} = 9$  Hz, Ph<sub>meta</sub>); 133.4 (d,  $J_{\text{CP}} = 4$  Hz, C<sub>h</sub>); 129.6 (Ph<sub>para</sub>); 129.5 (Ph<sub>para</sub>); 127.9 (d,  $J_{\text{CP}} = 11$  Hz, Ph<sub>ortho</sub>); 127.5 (d,  $J_{\text{CP}} = 11$  Hz, Ph<sub>ortho</sub>); 132.2 (dd,  $J_{\text{CP}}(\text{cis}) = 12$  Hz,  $J_{\text{CP}}(\text{trans}) = 98$  Hz, C–Ir); 114.4 (d,  $J_{\text{CP}} = 8$  Hz, C<sub>b</sub>); 105.5 (C<sub>g</sub>); 105.4 (C<sub>d</sub>). IR (Nujol,  $\text{cm}^{-1}$ ): 2473 ( $\nu_{\text{BH}}$ ), 2179 ( $\nu_{\text{IrH}}$ ).

**Acetonitrile Complex (3).** **1-*d*<sub>30</sub>** (10 mg, 0.01 mmol) was dissolved in  $\text{CD}_3\text{CN}$  (0.5 mL) in an NMR tube and flame sealed under vacuum. A new Tp complex and free  $\text{PPh}_3$ -*d*<sub>15</sub> were observed to grow in. The new complex was assigned the formula (*N,C<sup>5</sup>,N-Tp-H*)IrH(PPh<sub>3</sub>)(CD<sub>3</sub>CN) (CD<sub>3</sub>CN trans to the Ir–C).  $^1\text{H}$  NMR (500 MHz,  $\text{CD}_3\text{CN}$ ): 7.79 (d, 1H, H<sub>e</sub>); 7.73 (m, 1H, H<sub>h</sub>); 7.71 (m, 1H, H<sub>i</sub>); 7.28 (d, 1H, H<sub>c</sub>); 6.75 (d, 1H, H<sub>a</sub>); 6.18 (dd, 1H, H<sub>g</sub>); 6.02 (t, 1H, H<sub>d</sub>); 4.65 (d, 1H, H<sub>b</sub>); –19.3 (d,  $J_{\text{HP}} = 22$  Hz, 1H, Ir–H).  $^{13}\text{C}\{^1\text{H}\}$ : 142.1 (C<sub>h</sub>), 141.1 (C<sub>h</sub>), 138.0 (C<sub>a</sub>), 134.1 (C<sub>e</sub>), 133.5 (C<sub>f</sub>), 121.8 (d,  $J_{\text{CP}} = 12$  Hz, Ir–C), 113.2 (C<sub>b</sub>), 105.2 (C<sub>g</sub>), 104.9 (C<sub>d</sub>).  $^{31}\text{P}\{\text{aromatic } ^1\text{H}\}$ : 11.2 (d,  $J_{\text{PH}} = 22$  Hz).

**Reaction of ClIr(PPh<sub>3</sub>)<sub>3</sub> with KTP.** ClIr(PPh<sub>3</sub>)<sub>3</sub> (5 mg, 4.9 mmol) and KTP (1.2 mg, 5 mmol) were combined in an NMR

tube.  $\text{CD}_2\text{Cl}_2$  (0.5 mL) was added via vacuum transfer, and the tube was flame sealed. The reaction lightened from orange after 1 h and was almost colorless after 6 h. This reaction was accompanied by the appearance of several unidentified resonances in both the  $^{31}\text{P}$  and  $^1\text{H}$  NMR.

**Solid-State Structure of 2.** Crystals were grown as described above and mounted on glass capillaries in oil. Diffraction measurements were made on a prismatic crystal of dimensions  $0.20 \times 0.19 \times 0.09$  mm in a nitrogen stream at 161 K on a Nonius KappaCCD diffractometer using graphite-monochromated radiation ( $\lambda = 0.71070$  Å). Crystal-to-detector distance was 27 mm and exposure time was 15 s for all sets. The scan width was  $1^\circ$ . Data collection was 93.3% complete to  $30.53^\circ$  in  $2\theta$ . A total of 60 615 partial and complete reflections were collected covering the indices  $h = -12$  to 14,  $k = -20$  to 18,  $l = -23$  to 22. A total of 13 728 reflections were symmetry independent, and the  $R_{\text{int}} = 0.0411$  indicated good data quality. Indexing and unit cell refinement, based on 896 reflections, indicated a triclinic lattice. The space group was  $P\bar{1}$  (No. 2) with cell parameters  $a = 10.79070(10)$  Å,  $b = 14.0978(2)$  Å,  $c = 16.2606(2)$  Å;  $\alpha = 86.2246(6)^\circ$ ,  $\beta = 77.5581(8)^\circ$ ,  $\gamma = 85.0293(8)^\circ$ . The cell volume was  $2403.64(5)$  Å<sup>3</sup>, and the calculated density was  $1.461$  g/cm<sup>3</sup>. Solution by Patterson methods (DIRDIF) produced a complete heavy atom phasing model consistent with the proposed structure. Difference Fourier synthesis revealed a peak  $1.37$  Å from the iridium, assigned as a hydride. It was refined with isotropic thermal parameters to a distance of  $1.52(7)$  Å. All other hydrogen atoms were placed with idealized geometry except for H1B (boron hydrogen) and were refined with a riding model.  $U_{\text{iso}}$  values were fixed such that they were  $1.1U_{\text{eq}}$  of their parent atom and  $1.5U_{\text{eq}}$  for the acetonitrile methyl hydrogens. All non-hydrogen atoms were refined anisotropically by full matrix least squares. Large thermal displacement was noted for C35, C36, C37, and C47, indicating disorder. Splitting these atoms into two discrete sites did not improve the model. Correction for absorption was performed using a face-indexed procedure. Faces and distances to the center of the crystal used were  $\{100\}$  0.80 mm,  $\{010\}$  0.055 mm,  $\{001\}$  0.075 mm,  $\{011\}$  0.044 mm. Faces related by inversion were also present. Refinement proceeded to a final  $R = 4.05\%$ ,  $R_w = 14.19\%$  (GOF = 1.064).

**Acknowledgment.** This work was supported by the National Science Foundation. We are grateful for fellowship support (W.J.O.) from the Chevron Research and Technology Co. We acknowledge NSF support (CHE-9710008) of a 500 MHz spectrometer upgrade.

**Supporting Information Available:** Structure determinations for  $\text{TpIr}(\text{C}_2\text{H}_4)$  and **2**, ORTEP drawings, tables of positional and thermal parameters, and bond distances and angles. This material is available free of charge via the Internet at <http://pubs.acs.org>.

OM990720I